
**Liquid Crystals**
Publication details, including instructions for authors and subscription information:
http://www.informaworld.com/smpp/title~content=t713926090

# Fourier transform infrared study of two truxene-based discotic liquid crystals

Wah Keat Lee[a]; Paul A. Heiney[a]; Masashi Ohba[bc]; John N. Haseltine[bd]; Amos B. Smith III[b]
[a] Department of Physics and Laboratory for Research on the Structure of Matter, University of Pennsylvania, Philadelphia, Pennsylvania, U.S.A. [b] Department of Chemistry and Laboratory for Research on the Structure of Matter, University of Pennsylvania, Philadelphia, Pennsylvania, U.S.A. [c] Faculty of Pharmaceutical Science, Kanazawa University, Kanazawa, Japan [d] Department of Chemistry, Yale University, Connecticut, U.S.A.

**To cite this Article** Lee, Wah Keat , Heiney, Paul A. , Ohba, Masashi , Haseltine, John N. and Smith III, Amos B.(1990) 'Fourier transform infrared study of two truxene-based discotic liquid crystals', Liquid Crystals, 8: 6, 839 — 850
**To link to this Article: DOI:** 10.1080/02678299008047394
**URL:** http://dx.doi.org/10.1080/02678299008047394

LIQUID CRYSTALS, 1990, VOL. 8, NO. 6, 839–850

# Fourier transform infrared study of two truxene-based discotic liquid crystals

by WAH KEAT LEE and PAUL A. HEINEY

Department of Physics and Laboratory for Research on the Structure of Matter, University of Pennsylvania, Philadelphia, Pennsylvania 19104, U.S.A.

MASASHI OHBA†, JOHN N. HASELTINE‡ and AMOS B. SMITH, III

Department of Chemistry and Laboratory for Research on the Structure of Matter, University of Pennsylvania, Philadelphia, Pennsylvania 19104, U.S.A.

(*Received 9 May 1990; accepted 22 June 1990*)

We have used FTIR absorption to study the crystalline and liquid-crystalline phases of 2,3,7,8,12,13-hexa-*n*-tetradecanoyloxy-truxene (HATX) and 2,3,7,8,12,13-hexa(4-*n*-undecyloxybenzoyloxy)truxene (HBTX). Both materials show pronounced changes in the $CH_2$ stretching mode frequencies at their melting points. In addition, HATX shows a transition at about 20°C below the nominal melting point in which the alkyl tails gain significant disorder. Benzene stretching modes and the $CH_2$ deformation modes show subtle changes at the $D_{rd} \rightarrow N$ transition of HBTX and at the $D_{rd} \rightarrow D_{hd}$ transition of HATX.



## 1. Introduction

Molecules forming discotic nematic and columnar liquid crystals generally consist of a rigid, planar core with four or more flexible aliphatic tails. While it is clear that the anisotropy of the molecular shape (disc-like rather than rod-like) is crucial in determining the symmetry of the mesophase structure, the aliphatic tails also play an important role [1–5]. To our knowledge, discotic columnar phases have only been observed in materials with flexible tails. Based on X-ray diffraction measurements, we previously suggested [5] that temperature-driven tail disorder might be responsible for some of the inverted and reentrant phase sequences that have been observed in truxene-based discotics [5–10].

While optical microscopy and X-ray diffraction are the primary tools used in phase identification, dynamic probes such as Raman scattering, nuclear magnetic resonance (NMR) and infrared absorption are highly sensitive to local structure and motions of liquid crystal molecules. We have found that Raman scattering studies are complicated with the high degree of luminescence from these materials. Accordingly, we have used Fourier transform infrared (FTIR) absorption to study the vibrational dynamics of two truxene-based liquid crystals (2,3,7,8,12,13-hexa-*n*-tetradecanoyloxy-truxene (HATX) and 2,3,7,8,12,13-hexa(4-*n*-undecyloxybenzoyloxy) truxene (HBTX)) as a function of temperature. The molecular structures of these

† Present address: Faculty of Pharmaceutical Science, Kanazawa University, Takara-Machi, Kanazawa, Japan.

‡ Present address: Department of Chemistry, Yale University, New Haven, Connecticut 06511, U.S.A.

0267-8292/90 $3.00 

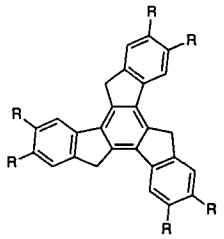

HATX: R = $CH_3(CH_2)_{12}COO$-

HBTX: R = $CH_3(CH_2)_{10}O$- 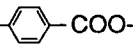 -COO-

Figure 1. Molecular structure of HATX and HBTX.

compounds are shown in figure 1. The object of this study was to gain an understanding of the local atomic positions within the molecule and the stabilization effect of tail disorder, in the various thermodynamic phases. In a related paper [11], we report FTIR measurements on a triphenylene based discotic liquid crystal, whose $D_{ho}$ phase exhibits helical order and a three column superlattice.

The phase sequences originally reported by Destrade *et al.* [9] for the compounds of interest were as follows:

For HATX:

$$C \xleftrightarrow[61°C]{} N_D \xleftrightarrow[84°C]{} D_{rd} \xleftrightarrow[112°C]{} D_{ho} \xleftrightarrow[241°C]{} I,$$

$$D_{ho} \xleftarrow{56°C}$$

For HBTX:

$$C \xrightarrow[90°C]{} D_{rd} \xleftrightarrow[137°C]{} N_D \xleftrightarrow[179°C]{} D_{rd} \xleftrightarrow[284°C]{} N_D \xleftrightarrow[297°C]{} I.$$

Here C is a crystalline phase, $N_D$ is the nematic phase, I is an isotropic phase, and D is a discotic columnar phase. Perhaps the most intriguing feature of these compounds is the fact that a reentrant *isotropic* phase is seen in mixtures of HATX with $\sim 13$ per cent HBTX [5, 9, 12].

An X-ray diffraction study of suspended strands of HATX [4] indicated that the high temperature phase should in fact, be classified as $D_{hd}$ (hexagonal disordered) rather than as $D_{ho}$ (hexagonal ordered), i.e. within the columns the molecules only have short-range positional order. These X-ray measurements also showed no sign of the reported $D_{ho}$–$D_{rd}$ transition at 112°C: the intensities of any low-temperature rectangular symmetry peaks were reduced from those of the hexagonal symmetry peaks by a factor of at least $10^4$, and the distortion of the column two dimensional lattice, which breaks the hexagonal symmetry, was determined to be less than 0·5 per cent.

Although we have not succeeded in growing single crystals of HATX or HBTX for structural analysis of the low-temperature C phase, we have made measurements of the X-ray *powder* profiles of these materials as a function of temperature; some of these measurements were reported in [5]. Analysis of these measurements has been complicated by partial (and non-reproducible) orientation of the powders. Nevertheless, the powder diffraction data show a number of significant features.

The diffraction peaks of both HATX and HBTX remain sharp up to the reported melting temperatures, indicating that crystalline long range order is preserved. In addition to the sharp crystalline Bragg peaks, a broad diffuse maximum is also observed at large angles. In the case of HATX, the maximum is centred at around $1{\cdot}5\,\text{Å}^{-1}$ at low temperatures, with a full width at half-maximum (FWHM) of about $0{\cdot}45\,\text{Å}^{-1}$. At the melting point, this diffuse peak moves down to about $1{\cdot}35\,\text{Å}^{-1}$, but retains its original width and intensity. In all the phases of HBTX below 106°C, including the crystalline phase, there is a broad peak at around $1{\cdot}4\,\text{Å}^{-1}$ with FWHM of about $0{\cdot}4\,\text{Å}^{-1}$. These broad features are associated with tail disorder [4]; they could result from either static or dynamic deviations from perfect crystalline order (elastic incoherent or thermal diffuse scattering).

The HATX powder diffraction data show a dramatic qualitative change at about 50°C during heating from room temperature. Warmderdam *et al.* [13] observed complex and strongly history-dependent optical calorimetric sequences below 80°C in HATX. They inferred that the C phase does not melt directly into the nematic phase, but rather that there is an intermediate columnar D phase. They also suggested that a virgin sample might consist of a mixture of two crystalline phases (C and C′), with the C phase partially melting at 56°C followed by crystallization into the C′ phase. Our powder X-ray studies do not support the existence of a pure D phase between 53°C and 60°C, but they are consistent with a transition between two thermodynamic states, each of which could consist of either a pure crystalline phase or coexistence between several crystalline or liquid-crystalline-columnar phases.



## 2. Physical measurements

Our samples were from the same batches as those studies by Fontes *et al.* [4] and Lee *et al.* [5]; the synthesis of these materials has been described previously [5]. About 10 mg of sample were dissolved in 0·4 ml of basic alumina-filtered chloroform. Using a syringe, a few drops of the solution were carefully deposited on a 25 mm diameter × 2 mm thick KBr disc at room temperature. Argon gas was passed over the drops to evaporate the solvent. This was repeated several times until about 2 mg of pure sample was deposited on the plate. To ensure complete evaporation of the solvent, the KBr plate was placed in a drying oven (80°C) for 3–5 min. A 0·015 mm thick teflon gasket was placed on the rim of the disc, and another clean KBr disc was seated above it to form the FTIR cell. The cell was placed in a Wilmad No. 118-3 cell mount attached to a Wilmad No. 0106 temperature controller. The temperature was stable to within 1°C. In order to obtain as uniform a thin film as possible, the cell was heated to about 100°C while the cell mount was carefully screwed in place, thereby pressing the two KBr plates together. In this way, the teflon gasket also formed a seal, preventing the sample from leaking. The cell was then allowed to cool back to room temperature.

All infrared absorption measurements were done on an IBM IR/97 FTIR instrument in transmission mode. The sample compartment was purged with dried nitrogen gas for at least 3 hours before data collection. A total of 128 scans were co-added to give a reasonable signal-to-noise ratio such that the smaller peaks were resolved. Scans were taken in the 400 to 4000 $\text{cm}^{-1}$ region, with a total of 14 934 points per scan, and a resolution of $0{\cdot}5\,\text{cm}^{-1}$. A reference spectrum of empty KBr disks was taken and was used for subsequent computation of the absorption spectra. As a check, several spectra of the reference cell were taken at different temperatures ranging from 30°C

to 175°C. There were no observable differences between these spectra. Data were taken in 5°C increments by heating the sample from 29°C to 187°C.

In order to study the evolution of the IR peaks quantitatively, we performed least-squares fits to a model consisting of a sum of lorentzian functions and a quadratic background function. It was occasionally necessary to parameterize a single peak with more than one lorentzian. In these cases, we quote the weighted average of the various sub-frequencies. Due to possible sample flow within the FTIR cell, we cannot be sure that the IR beam passes through the same amount of sample as the cell is heated. Therefore, in interpreting the results of our analysis, we concentrate mainly on the frequency changes rather than amplitude changes.

## 3. Measurements on HATX

Figures 2 (i) and (ii) show the FTIR absorption scans of HATX taken at 29°C and 169°C. The data in the 400 to 600 $cm^{-1}$ region have been truncated due to the rapidly increasing noise levels near 400 $cm^{-1}$. Based on previous infrared studies [14–17], several peaks are identified as follows: (*a*) CH stretching modes near 2900 $cm^{-1}$, (*b*) C=O stretching mode near 1760 $cm^{-1}$, (*c*) benzene stretching modes near 1600 $cm^{-1}$, (*d*) CH deformation modes near 1470 and 1380 $cm^{-1}$, (*e*) out-of-plane single aromatic hydrogen bending mode near 875 $cm^{-1}$, and (*f*) CH rocking mode of the methylene chain near 720 $cm^{-1}$. The bands near 1270 and 1160 $cm^{-1}$ are probably

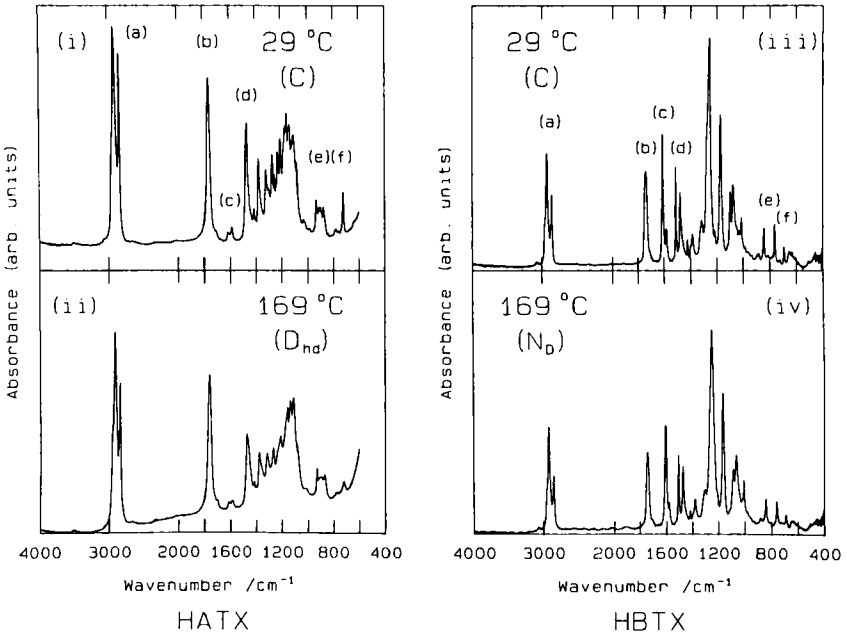


Figure 2. Complete FTIR absorption spectra of HATX at (i) 29°C, (ii) 169°C, and HBTX at (iii) 29°C, and (iv) 169°C. The spectrum for HATX has been truncated in the 400 to 600 $cm^{-1}$ region due to increasing noise levels near 400 $cm^{-1}$. The bands in the marked regions are assigned as follows: (*a*) methyl and methylene CH stretches, (*b*) carbonyl C=O stretches, (*c*) benzene ring breathing modes, (*d*) methyl and methylene CH bends and scissoring, (*e*) out-of-plane deformation of aromatic hydrogen, and (*f*) methylene rocking mode. Other bands have no definite assignments. Note the compressed scale from 4000 to 2000 $cm^{-1}$.

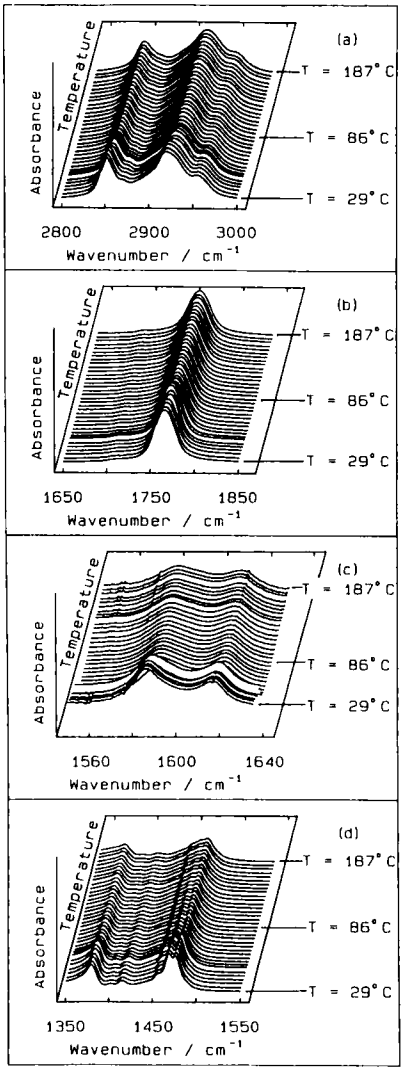


Figure 3. HATX FTIR absorption profiles of (*a*) CH stretching modes, (*b*) C=O stretching modes, (*c*) benzene stretching modes, and (*d*) CH bending/scissoring modes at different temperatures. Data were taken upon heating to the following temperatures: 29, 33, 39, 43, 53, 58, 63, 68, 72, 77, 81, 86, 91, 100, 105, 109, 114, 118, 123, 127, 132, 136, 141, 146, 151, 155, 160, 164, 169, 173, 178, 182 and 187°C. The plots have arbitrary and different vertical scales.

due to O=C–O and C–O–C stretching modes, although, due to the proximity of the peaks, individual modes could not be identified with confidence. The two spectra are clearly quite similar; with increasing temperature, peaks tend to lose intensity and to broaden, so that nearby peaks become unresolved.

Figure 3 shows the evolution of selected individual absorption peaks with increasing temperature. In figure 3 (*a*), the two main peaks near 2855 and 2923 $cm^{-1}$ are due to the symmetric and asymmetric stretching modes of $CH_2$ respectively. The peak shoulders near 2870 and 2955 $cm^{-1}$ are due to the symmetric and asymmetric stretching modes of $CH_3$ respectively. Figure 3 (*b*) shows the carbonyl C=O stretching bands.

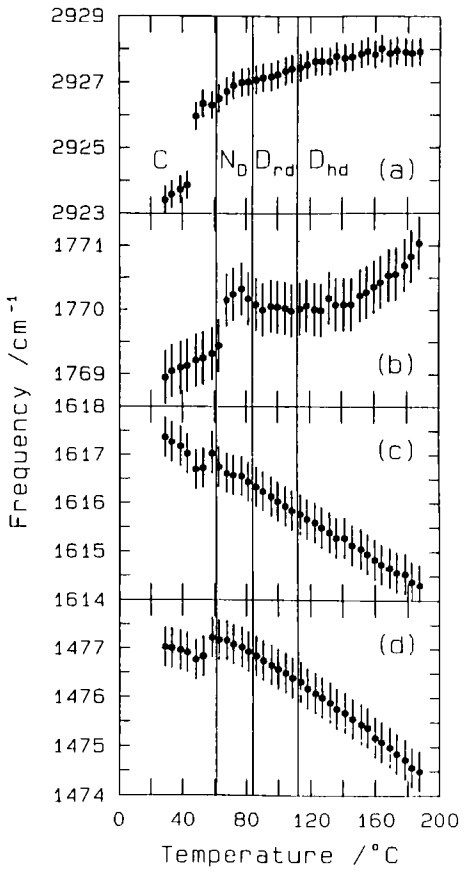


Figure 4. Fitted positions of the HATX absorption peaks from lorentzian fits: (*a*) methylene asymmetric CH stretching mode, (*b*) carbonyl C=O stretching mode, (*c*) benzene stretching mode, and (*d*) methylene scissoring mode. In cases where more than one lorentzian were needed to give a reasonable fit, the weighted average of the positions are plotted. Data were taken by heating the sample from ~ 29°C to ~ 187°C in 5°C increments. Error bars indicate estimated errors from the fits. Vertical lines show the phase boundaries from previous studies.

Kardan *et al.* [18] have observed that the carbonyl stretching bands of a benzene hexa-*n*-alkanoate discotic liquid crystal is actually made up of two different bands, due to two possible different orientations of the C=O bond relative to the neighboring C–C bond. In our attempts to model this peak, we find that we actually needed three bands (i.e. three lorentzian profiles as discussed above) to get a reasonable fit. Both bands in figure 3(*c*) are assigned to benzene stretching modes. The band near 1380 cm$^{-1}$ in figure 3(*d*) is most likely due to the symmetric bending mode of $CH_3$, while the bands near 1468 and 1477 cm$^{-1}$ are most likely due to the asymmetrical bending of $CH_3$ and the scissoring mode of $CH_2$ respectively, although we note that the latter two appear to be centred about 10 cm$^{-1}$ higher than the position that is normally observed for *n*-alkanes [16, 17].

In figure 4, we plot the frequencies of various modes extracted from least squares fits to lorentzian profiles. Figure 4(*a*) shows the weighted average of the methylene asymmetric CH stretching frequencies as a function of temperature. Note the large

jump in the absorption frequency at about 45°C, and a change in the slope at about 65°C. From 65°C onwards, the absorption frequency appears to increase slowly with increasing temperature, with a slight levelling off at about 160°C. Figure 4 (*b*) shows the carbonyl C=O stretching frequency as a function of temperature. A jump in frequency is seen at about 62°C, and the slope changes at about 150° C. The frequency of a benzene breathing mode is shown in figure 4 (*c*). Changes in slope are seen at around 45°C and 62°C. Finally, the $CH_2$ scissoring bending mode frequency is shown in figure 4 (*d*). Changes in slope can be seen at around 45°C, 62°C, 110°C and 150°C.

Asher and Levin [19] and Snyder *et al.* [20] have shown that the CH stretching frequencies are primarily sensitive to the chain conformation and that their absorption frequencies increase in the presence of nearby *gauche* bonds [21, 22]. Therefore, we interpret the sudden increases in absorption frequency, seen in figure 4 (*a*), as sudden increases in the statistical distribution of *gauche* bonds on the alkyl tails of the HATX molecule. The presence of substantial tail disorder is consistent with the large-angle diffuse scattering seen in the X-ray powder patterns. It is interesting to note that the large increase in the absorption frequency occurs near 45°C, 20°C *lower* than the melting transition temperature. Thus, the tail disorder increases abruptly and significantly well below the $C-N_D$ transition, an effect that has been previously seen in compounds such as benzene hexa-*n*-alkanoates [18] and hexahydroxybenzene hexaoctanoate [23]. This 'pre-melting' effect has been observed on two independent measurements of two different HATX sample cells. It could either result from a true thermodynamic transition between two solid phases, in which the tails collectively become more disordered at a well-defined transition temperature, or merely a rapid but continuous evolution of tail disorder which acts as a precursor to the actual melting transition. As discussed in the introduction, our X-ray data are consistent with solid–solid phase transition; however, a non-equilibrium 'double melting' transition as suggested by Warmerdam *et al.* cannot be ruled out.

On heating the sample above the melting temperature, the CH stretching frequency undergoes a small gradual increase, and plateaus at about 160°C. Thus, any increases in the statistical distribution of *gauche* bonds in the alkyl tails upon heating after the melting temperature must be quite small. This levelling out of the CH stretching frequency at the melting temperature is similar to that seen by Cameron *et al.* working with 1,2-dipalmitoyl-*sn*-glycero-3-phosphocoline [24].

The C=O stretching band is best modelled by a sum of three lorentzians. The weighted average position of these peaks is plotted against temperature in figure 4 (*b*). The absorption frequency clearly jumps at the melting temperature of 65°C. There is also a change in slope at around 150°C. Kardan *et al.* [18] have also observed such an increase in the C=O stretching frequency in the melting transition of benzene hexa-*n*-alkanoates. They have suggested that this could be due to the molecular cores moving apart upon melting. We are currently undertaking computer simulations in order to understand further the core–core interactions of the different phases. There do not appear to be any anomalies in the data at around 45°C. Since the carbonyl bond is close to the truxene core, this again suggests that the observed pre-melting transition only involves the alkyl tails.

Figure 4 (*c*) shows the temperature dependence of a benzene stretching frequency. No significant features are seen beyond the anomaly of 45°C. The temperature dependence of the $CH_2$ scissoring mode is plotted in figure 4 (*d*). Anomalies are seen at about 45°C and 65°C. In addition, there appear to be small changes in slope at about 110°C and 150°C. As discussed above, optimal microscopy measurements

[6, 13] indicate a $D_r \rightarrow D_h$ transition at $\sim 112°C$, although no transition at 112°C was observed in the course of single-strand X-ray studies performed in our laboratory [4]. The present IR absorption data suggest that there is, in fact, some transition in the vicinity of 112°C, in which the alkyl tails undergo a subtle change in environment, without significant changes to the core or to the number of *gauche* bonds. X-ray diffraction intensities are expected to be fairly insensitive to small changes in tail conformation, because the tail–tail correlation peak is quite broad. Infrared absorption spectra of CH bending modes have been shown to be sensitive to alkyl chain conformation and to chain packing [25]. Any sliding or rotating of the alkyl chains with respect to the neighbouring chains might thus show up in the IR spectra, but not in the X-ray data. Therefore, the balance of evidence at this time indicates that there is a transition at 112°C, most likely from a $D_{rd}$ to $D_{hd}$ phase, which involves primarily motions of the alkyl tails rather than any motion of the cores.

Finally, we note that the absorption bands in the region 600 to 4000 $cm^{-1}$ do not show any anomaly at the $N \rightarrow D_{rd}$ (84°C) transition. Therefore, we conclude that this transition must involve only very subtle changes in the local environment. This is consistent with X-ray diffraction studies showing that the various liquid-crystalline phases have similar short-range order [1, 5].



## 4. Measurements on HBTX

Figures 2 (iii) and (iv) show the complete FTIR absorption scans of HBTX taken at 29°C and 169°C. Several peaks are identified as follows: (*a*) CH stretching bands near 2900 $cm^{-1}$, (*b*) carbonyl C=O stretching bands near 1735 $cm^{-1}$, (*c*) benzene ring stretching bands near 1600 and 1510 $cm^{-1}$, (*d*) CH deformation bands near 1480 and 1380 $cm^{-1}$, (*e*) single core-H out-of-plane bending bands near 840 and 760 $cm^{-1}$ and (*f*) $CH_2$ rocking bands near 720 $cm^{-1}$. The bands near 1250, 1170, 1090 and 1070 are probably due to O–C=O or C–O–C stretches, but due to the proximity of the peaks, individual modes could not be identified with confidence. Also, note that the intensities of the benzene stretching modes shown here are much higher than those of HATX. This is due to the additional benzoyl groups attached to the alkyl tails near the core. The two HBTX spectra taken at different temperatures are qualitatively similar. As in HATX, the amplitudes decrease and peaks broaden so that nearby peaks become unresolved with increasing temperature.

Figure 5 shows the variation of the absorption peaks at different regions with increasing temperature. Detailed band assignments for the different regions shown in figure 5 are identical to those of HATX. The only difference is that the carbonyl C=O stretching bands appears near 1738 $cm^{-1}$ and the benzene band appears near 1606 $cm^{-1}$.

Figure 6 (*a*) shows the temperature dependence of the $CH_2$ asymmetric stretching frequency. There is clearly a small break in the position and change in slope at around 85°C. There may also be a small change in slope at around 135°C. Figure 6 (*b*) shows the plot of the weighted average of the carbonyl C=O stretching frequency as a function of temperature. There is a sharp increase in the absorption frequency at about 85°C. The absorption frequency of a benzene stretching mode is plotted against temperature in figure 6 (*c*). An anomaly again is seen at around 85°C and a small change in slope at around 135°C. The $CH_2$ scissoring and the $CH_3$ asymmetric bending modes are unresolved in the HBTX spectra. The weighted average of their peak positions is plotted against temperature in figure 6 (*d*).

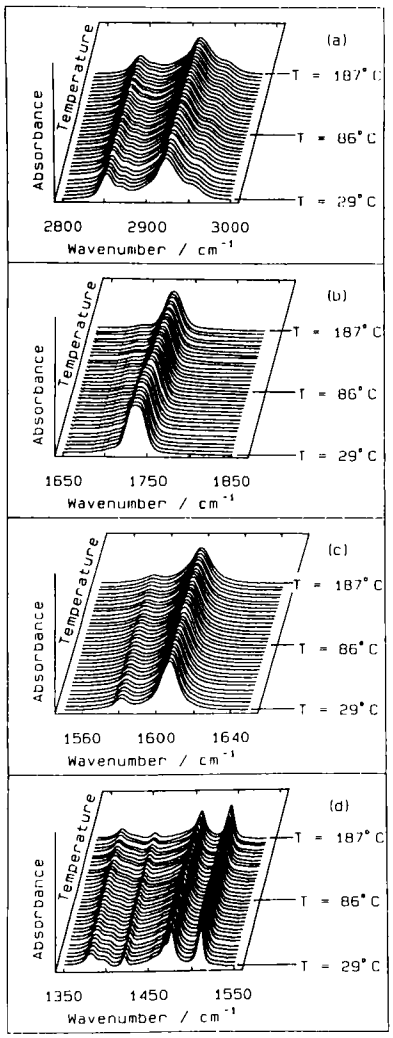


Figure 5. HBTX FTIR profiles of (*a*) CH stretching modes, (*b*) C=O stretching modes, (*c*) benzene ring stretching modes, and (*d*) CH bending/scissoring modes at different temperatures. Data were taken upon heating at the same temperatures as in figure 3. The plots have arbitrary and different vertical scales.

The temperature dependence of the CH stretching bands clearly suggests that even in the crystalline phase, the statistical distribution of *gauche* bonds in the alkyl tails increases significantly upon heating. The rate of increase decreases in the $D_{rd}$ phase and becomes small or zero near the $D_{rd} \rightarrow N$ transition. This is considerably different from the evolution in HATX, where two distinct transitions are observed. As is the case for HATX, the 1·4 $Å^{-1}$ diffuse peak observed in powder X-ray measurements of HBTX suggests that the alkyl tails of HBTX are significantly disordered even in the crystalline phase. This notion is supported by the IR data.

If we compare the CH stretching bands of HATX and HBTX as a whole, we see that the HBTX bands are at a higher frequency. Previous studies [19, 20] have shown that the CH stretching modes are quite insensitive to the environment except for the

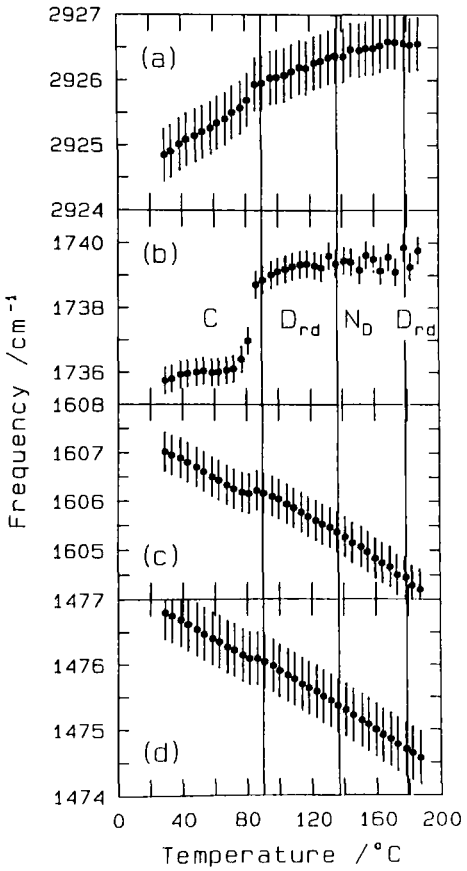


Figure 6. Fitted positions of the HBTX absorption peaks from lorentzian fits. (*a*) Methylene asymmetric CH stretching mode, (*b*) carbonyl C=O stretching mode, (*c*) benzene stretching mode, and (*d*) methylene scissoring mode. In cases where more than one lorentzian were needed to give a reasonable fit, the weighted average of the positions is plotted. Data were taken by heating the sample from ~ 29°C to ~ 187°C in 5°C increments. Error bars indicate estimated errors from the fits. Vertical lines show the phase boundaries from previous studies.

existence of nearby *gauche* bonds. Although comparisons of spectra from different molecules must be treated with caution, we can speculate that the tails of HBTX are more disordered than that of HATX.

The weighted average of the carbonyl C=O stretching frequency is plotted against temperature in figure 6 (*b*). The scatter in the data points gives an indication of the uncertainty due to the existence of multiple or shallow minima in the least-square fitting procedure. The only clearly identifiable feature is the large increase in absorption frequency near the melting temperature of 85°C. Again, we note that this band is best fitted by a sum of three lorentzians. As in the case of HATX, one might interpret the jump at 85°C as a sudden increase in the core–core distance upon melting.

In addition to an anomaly at the melting point near 85°C, the plot of a benzene stretching mode frequency versus temperature, figure 6 (*c*), shows a small, but detectable change in slope at about 135°C, corresponding to the $D_{rd} \rightarrow N$ transition. Since

this transition involves changes in the core–core interactions, and the benzoyl groups are attached near the core, it is not surprising that we see an anomaly in the benzene stretching frequency at this temperature. The $CH_2$ scissoring and the $CH_3$ asymmetrical bending bands are unresolved in the HBTX spectra. The weighted average frequency of these two bands is plotted against temperature in figure 6(*d*). We see an anomaly at about 85°C, and, as in HATX, we observe decreasing absorption frequency with increasing temperature.

## 5. Summary

Our results, together with previously published X-ray data, suggest the following microscopic picture for HATX. At about 20°C below the nominal melting point, there is a sudden increase in the statistical distribution of *gauche* bonds in the alkyl tails. This increase could result from a structural phase transition characterized primarily by tail 'melting', or the non-equilibrium annealing, or melting of a quenched crystalline phase. At the melting point, the rate of increase of *gauche* bond density decreases. Further heating past the melting point only increases the number of *gauche* bonds in a very gradual fashion. No changes were observed at the $N \rightarrow D_{rd}$ transition. A very small change in the CH bending frequency at 112°C suggests that the $D_{rd} \rightarrow D_{hd}$ transition may primarily involve tail, rather than core configurations. Changes in the C=O stretching and the CH bending frequencies suggest that there may also be small changes in the core and tail environments at around 150°C.

For HBTX, the microscopic picture is as follows. The crystalline phase gradually develops an increasing number of *gauche* bonds as the temperature is increased. This increase continues into the columnar phase at a slower rate. The $D_{rd} \rightarrow N$ transition appears to affect the truxene core only and does not increase the number of *gauche* bonds significantly.

We have also measured IR spectra of *mixtures* of HATX with 9·83 mol % HBTX. To within 50 per cent in intensity, all features appear to be the sums of peaks in the respective IR patterns of the two compounds individually. The thermal evolution is qualitatively similar to that observed for pure HATX and HBTX. Large changes are seen in the CH stretching modes and the C=O stretching modes at the melting temperature. No change is seen in the reentrant isotropic ($I \leftrightarrow D + 1 \leftrightarrow I$) sequence observed by other techniques, indicating that the local order must remain essentially unchanged through this region.

We thank George Furst and John Brahms for their technical assistance. We also thank Professors Eugene Nixon and William Dailey for help in interpreting the complex IR spectra. This work was supported by the National Science Foundation Grants DMR MRL 88-19885 and DMR 89-01219.

## References

[1] Levelut, A. M., 1983, *J. Chim. phys.*, **80**, 149.
[2] Dowell, F., 1983, *Phys. Rev.* B, **28**, 3526.
[3] Yang, X., Waldman, D. A., Hsu, S. L., Nitzche, S. A., Thakur, R., Collard, D. M., Lillya, C. P., and Stidham, H. D., 1988, *J. chem. Phys.*, **89**, 5950.
[4] Fontes, E., Heiney, P. A., Ohba, M., Haseltine, J. N., and Smith, A. B., 1988, *Phys. Rev.* A, **37**, 1329.
[5] Lee, W. K., Wintner, B. A., Fontes, E., Heiney, P. A., Ohba, M., Haseltine, J. N., and Smith, A. B., 1989, *Liq. Crystals*, **3**, 87.

[6] DESTRADE, C., MALTHÊTE, J., NGUYEN HUU TINH, and GASPAROUX, H., 1980, *Physics Lett.* A, **78**, 82.
[7] DESTRADE, C., GASPAROUX, H., BABEAU, A., NGUYEN HUU TINH, and MALTHÊTE, J., 1981, *Molec. Crystals liq. Crystals*, **68**, 37.
[8] NGUYEN HUU TINH, MALTHÊTE, J., and DESTRADE, C., 1981, *J. Phys. Paris*, **42**, L417.
[9] DESTRADE, C., FOUCHER, P., MALTHÊTE, J., and NGUYEN HUU TINH, 1982, *Physics Lett.* A, **88**, 187.
[10] WARMERDAM, T., FRENKEL, D., and ZIJLSTRA, R. J. J., 1988, *Liq. Crystals*, **3**, 149.
[11] LEE, W. K., HEINEY, P. A., OHBA, M., HASELTINE, J. N., and SMITH, A. B., *Molec. Crystals liq. Crystals* (submitted).
[12] Specifically, Destrade *et al.* [9], using optical microscopy, reported the existence of a reentrant isotropic phase in a mixture of 2,3,7,8,12,13-hexa(*n*-tetradecanoyloxy)-truxene (HATX) and 2,3,7,8,12,13-hexa(4-*n*-dodecloxybenzoyloxy)-truxene (**a**), and also reported a phase sequence for pure 2,3,7,8,12,13-hexa(4-*n*-undecyloxybenzoyloxy)-truxene (denoted HBTX in the present paper), which is the homologue of **a** with one fewer carbon per chain. Lee *et al.* [5] subsequently used optical microscopy and X-ray diffraction to study mixtures of HATX and HBTX, and reported a reentrant isotropic phase in these mixtures as well. Indeed, the two sets of mixtures appear to have essentially identical phase diagrams, aside from small differences in phase transition temperatures.
[13] WARMERDAM, T. W., NOLTE, R. J. M., DRENTH, W., VAN MILTENBURG, J. C., FRENKEL, D., and ZIJLSTRA, R. J. J., 1988, *Liq. Crystals*, **3**, 1087.
[14] SILVERSTEIN, R. M., BASSLER, G. C., and MORRILL, T. C., 1981, *Spectrometric Identification of Organic Compounds*, fourth edition (Wiley).
[15] SNYDER, R. G., 1960, *J. molec. Spectrosc.*, **4**, 411.
[16] SNYDER, R. G., and SCHACHTSCHNEIDER, J. H., 1963, *Spectrochim. Acta*, **19**, 85.
[17] SCHACHTSCHNEIDER, J. H., and SNYDER, R. G., 1963, *Spectrochim. Acta*, **19**, 117.
[18] KARDAN, M., REINHOLD, B. B., HSU, S. L., THAKUR, R., and LILLYA, C. P., 1986, *Macromolecules*, **19**, 616.
[19] ASHER, I. M., and LEVIN, I. W., 1977, *Biochim. biophys. Acta*, **468**, 63.
[20] SNYDER, R. G., HSU, H. L., and KRIMM, S., 1985, *Spectrochim. Acta* A, **34**, 395.
[21] CAMERON, D. G., CASAL, H. L., MANTSCH, H. H., BOULANGER, Y., and SMITH, I. C. P., 1981, *Biophys. J.*, **35**, 1.
[22] UMEMURA, J., CAMERON, D. G., and MANTSCH, H. H., 1980, *Biochim. Biophys. Acta*, **602**, 32.
[23] YANG, X., KARDAN, M., HSU, S. L., COLLARD, D., HEATH, R. B., and LILLYA, C. P., 1988, *J. phys. Chem.*, **92**, 196.
[24] CAMERON, D. G., CASAL, H. L., and MANTSCH, H. H., 1980, *Biochemistry*, **19**, 3665.
[25] SNYDER, R. G., 1967, *J. chem. Phys.*, **47**, 1316.